

# Tidal notches in Mediterranean Sea: a comprehensive analysis

Fabrizio Antonioli <sup>a</sup>, Valeria Lo Presti <sup>b, a, \*</sup>, Alessio Rovere <sup>c, d</sup>, Luigi Ferranti <sup>e</sup>,  
Marco Anzidei <sup>f</sup>, Stefano Furlani <sup>g</sup>, Giuseppe Mastronuzzi <sup>h</sup>, Paolo E. Orru <sup>i</sup>,  
Giovanni Scicchitano <sup>j</sup>, Gianmaria Sannino <sup>a</sup>, Cecilia R. Spampinato <sup>k</sup>, Rossella Pagliarulo <sup>l</sup>,  
Giacomo Deiana <sup>i</sup>, Eleonora de Sabata <sup>m</sup>, Paolo Sansò <sup>n</sup>, Matteo Vacchi <sup>o</sup>, Antonio Vecchio <sup>f</sup>

<sup>a</sup> ENEA, UTMEA, Casaccia, Roma, Italy

<sup>b</sup> Department of Earth Sciences, "Sapienza" University, Rome, Italy

<sup>c</sup> MARUM, University of Bremen & ZMT, Tropical Marine Ecology Center, Bremen, Germany

<sup>d</sup> Lamont-Doherty Earth Observatory, Columbia University, NY, USA

<sup>e</sup> Department of Earth Sciences, Environment and Resources, "Federico II" University, Napoli, Italy

<sup>f</sup> Istituto Nazionale di Geofisica e Vulcanologia, Roma, Italy

<sup>g</sup> Department of Mathematics and Geosciences, University of Trieste, Italy

<sup>h</sup> Department of Earth and Geoenvironmental Sciences, "Aldo Moro" University, Bari, Italy

<sup>i</sup> Department of Chemical and Geological Sciences, University of Cagliari, Italy

<sup>j</sup> Department of Physics and Earth Sciences, University of Messina, Italy

<sup>k</sup> Department of Biological, Geological and Environmental Sciences, University of Catania, Italy

<sup>l</sup> CNR, IRPI, Bari, Italy

<sup>m</sup> MedSharks, Roma, Italy

<sup>n</sup> Department of Biological and Environmental Sciences and Technologies, University of Salento, Lecce, Italy

<sup>o</sup> Aix-Marseille Université, CEREGE CNRS-IRD UMR 34, Europole de l'Arbois Aix-en-Provence, France

## ARTICLE INFO

Accepted 20 March 2015

### Keywords:

Tidal notches  
Mediterranean Sea  
Relative sea level rise  
Holocene

## ABSTRACT

Recent works (Evelpidou et al., 2012) suggest that the modern tidal notch is disappearing worldwide due sea level rise over the last century. In order to assess this hypothesis, we measured modern tidal notches in several of sites along the Mediterranean coasts. We report observations on tidal notches cut along carbonate coasts from 73 sites from Italy, France, Croatia, Montenegro, Greece, Malta and Spain, plus additional observations carried outside the Mediterranean. At each site, we measured notch width and depth, and we described the characteristics of the biological rim at the base of the notch. We correlated these parameters with wave energy, tide gauge datasets and rock lithology.

Our results suggest that, considering 'the development of tidal notches the consequence of midlittoral bioerosion' (as done in Evelpidou et al., 2012) is a simplification that can lead to misleading results, such as stating that notches are disappearing. Important roles in notch formation can be also played by wave action, rate of karst dissolution, salt weathering and wetting and drying cycles. Of course notch formation can be augmented and favoured also by bioerosion which can, in particular cases, be the main process of notch formation and development.

Our dataset shows that notches are carved by an ensemble rather than by a single process, both today and in the past, and that it is difficult, if not impossible, to disentangle them and establish which one is prevailing. We therefore show that tidal notches are still forming, challenging the hypothesis that sea level rise has drowned them.

## 1. Introduction

Marine tidal notches (hereafter MTNs) are indentations or undercuttings, few centimetres to several metres deep, cut in steep calcareous cliffs at or near sea level (Carobene, 1972; Pirazzoli, 1986; Kelletat, 2005). Although the measurement of tidal notches

\* Corresponding author. Department of Earth Sciences, Mineralogy-Geology Edifice (no. 5), Sapienza University, 5 Aldo Moro square, 00185, Roma, Italy.  
E-mail address: [valeria.lopresti@uniroma1.it](mailto:valeria.lopresti@uniroma1.it) (V. Lo Presti).

in the field is trivial and can be done using simple instruments such as a stick metre, two aspects in the study of notches remain challenging. The first is the understanding of the mechanisms of their formation, which can be ascribed to chemical dissolution processes in the intertidal zone, wetting and drying cycles, biological erosion or wave action or, most likely, a combination of these factors. The second is that notches cannot be dated directly, and the estimate of their age relies, in the best cases, on the dating of organisms that form the biological rim covering part of the notch (Pirazzoli et al., 1994; Faivre et al., 2013) or correlating the elevation of a notch with other datable markers. In the worst cases, relative age estimates can be obtained comparing notch (bio)erosion rates and the dimensions of the notch.

Due to the difficulty in establishing the age of MTNs, there is an ongoing debate regarding their origin. The classical view is that MTNs are shaped around mean sea level and each time that a MTN is found out of the tidal range, or each time its shape deviates from the typical half-ellipsoidal shape (Carobene, 1972; Pirazzoli, 1986), there has been either a rapid (co-seismic or volcano-tectonic) or a gradual (e.g. due to regional tectonic processes) land movement. To this view, some authors (Cooper et al., 2007; Evelpidou et al., 2012) countered a model where formation of notches can happen only during periods of relative climatic and sea level stability, when bioerosion can 'keep up' with the pace of sea level rise.

Based on areas located in Greece (coasts of the Corinth Gulf, the Euboean Gulf and several Cyclades islands), Evelpidou et al. (2012) stated that: *'The most recent continuous sea level rise has resulted to the absence of a present-day notch'*.

Building on this hypothesis, Pirazzoli and Evelpidou (2013) state that present-day tidal notches are not forming anymore near sea level, while a 'fossil' tidal notch (developed before the sea level rise of 19th and 20th century) is often found between –20 and –65 cm below present sea level. They assert that *'present-day tidal notches are worth being re-measured and re-interpreted'*. One consequence of their hypothesis is that, if proved, tidal notches would lose most of their significance as markers of more or less rapid tectonic movements. Boulton and Stewart (2014) addressed this discussion by analysing a database of Holocene tidal notches dated using radiocarbon ages on fossil incrustation on the notch. They showed that the notches are not clustered around any known period of climatic stability as it would be expected if the hypothesis advanced by Cooper et al. (2007) is valid.

This ongoing debate, coupled to the observation of the presence, along the world's stable sedimentary carbonate coasts, of modern tidal notches, stimulated the collaboration of the group of researchers authoring this paper. We performed a reassessment of notches that are located near present sea level at 73 sites distributed along many carbonate coasts of the Mediterranean Sea (Fig. 1a; S1 supplementary material, hereafter SM). These sites were selected because their relative tectonic stability has been postulated on the basis of independent markers, most often the elevation of the Last Interglacial shoreline (MIS 5e, ~125 Ka ago, Ferranti et al., 2006, and references therein). We collected in-situ observations and measurements of the morphology of MTNs along the coasts of Croatia, France, Greece, Italy, Malta, Montenegro and Spain. In addition, we incorporate observations carried at 5 stable sites outside the Mediterranean Sea.

At each site we measured the different elements of MTNs and the presence, thickness and characteristics of the algal rim, as well as the lithological composition of the limestone. We then compare the measured notches and the thickness of the algal rims to wave energy and tidal ranges, to contribute to the understanding of notch formation. In this paper we show the implications of our results in terms of processes contributing to the shaping of tidal notches and relationship between tidal notches and sea level.

## 2. Notches in the Mediterranean: relevant aspects

### 2.1. Geologic context of the Mediterranean basin

The Mediterranean area marks the broad convergent boundary between the African and the Eurasian plates. The geodynamic characteristics of this region are dictated by lithospheric blocks showing different structural and kinematic interaction, including collision, subduction, back-arc spreading, and fold-and-thrust belt development. The complexity of the orogen is attributable in large part to the original geometry of the opposing plate margins and the existence of continental blocks within the western Tethys (Channell and Horvath, 1976; Jolivet and Faccenna, 2000; Serpelloni et al., 2007; Royden and Papanikolaou, 2011, Fig. 1b).

The coasts straddling the Mediterranean orogenic belts are characterized by a variable pattern of long-to short-term vertical tectonic motion, as documented by the elevation of ancient strandlines (Ferranti et al., 2006, 2010). An estimate of the stability of Mediterranean coastal areas can be derived from geomorphological indicators of the Holocene and of the Last Interglacial shoreline position. From these data it is evident that many sectors of the Mediterranean Sea exhibit significant vertical tectonic movements at least since MIS 5.5 and up to the recent (Ferranti et al., 2006, 2010) (Fig. 1c). Conversely, others sectors can be considered stable or affected by very low tectonic motions; these last are the areas studied in this work. Stratigraphic, morphological paleontological, archaeological and chronological data (Flemming and Webb, 1986; Pirazzoli, 1991; Antonioli et al., 2009; Ferranti et al., 2010; Vacchi et al., 2012; Sulli et al., 2013; Anzidei et al., 2011; 2014), indicate that, in general, the western Mediterranean coasts can be considered tectonically stable in the last 125 ka, while large sectors of Italy, Greece and Turkey are characterized by rapid transitions between subsiding, uplifting or stable coasts during the same span of time. On the other hand, stability or low tectonics characterize in general the coasts of North Africa for which published paleo shorelines exist.

### 2.2. Climate, waves, hydrological conditions and tides

Enclosed between the storm belt of northern Europe and the tropical area of northern Africa, the Mediterranean has a relatively mild climate on the average, but substantial storms are possible, usually in the winter months (Cavaleri et al., 1991; Cavaleri, 2000). The Mediterranean winter climate is dominated by the westward movement of storms originating over the Atlantic and impinging upon the western European coasts, the maximum measured significant wave height reaches 10 m, but model estimates for some non-documented storms suggest larger values (Giorgi and Lionello, 2008). Furthermore, Mediterranean storms can be produced within the region in cyclogenetic areas such as the lee of the Alps, the Gulfs of Lyon and Genoa; moreover, the number of exceptional storms linked to Tropical-Cyclones generated in Southern Mediterranean region is recently increasing (Lionello et al., 2006; Rebora et al., 2013). High pressure and descending motions dominate instead during the summer period, leading to dry conditions particularly in the southern Mediterranean.

The summer Mediterranean climate variability has been found to be connected with both the Asian and African monsoons and with strong geopotential blocking anomalies over central Europe (Alpert et al., 2006; Giorgi et al., 2008). The coasts of Mediterranean Sea are genetically connected to the presence of extended catchments shaped on carbonatic rocks. As such, they are largely characterized by karst groundwater springs, that reach the surface both above or below mean sea level. Such springs have been inferred to influence the development of marine notches (Higgins, 1980;

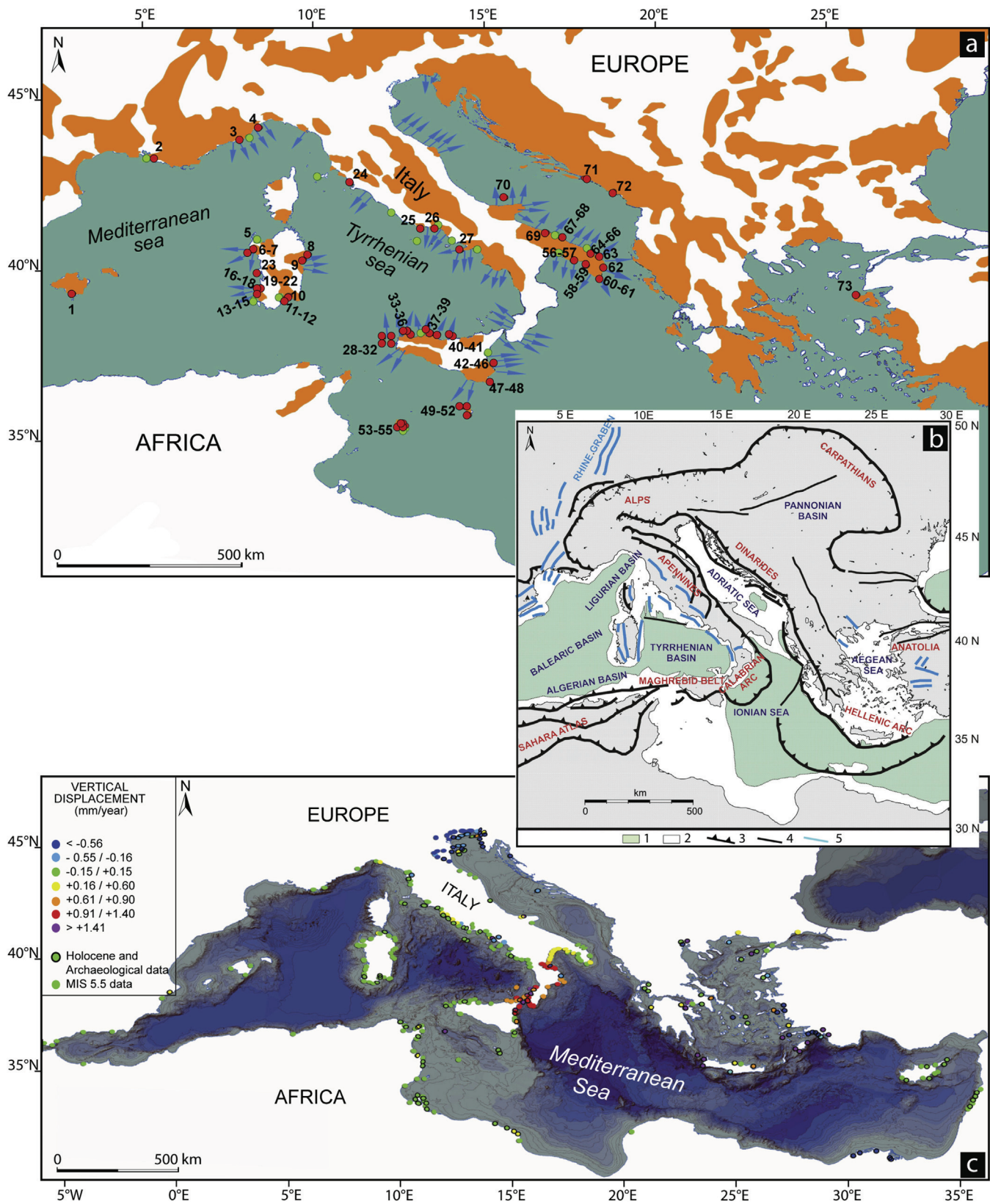


**Fig. 1.** **a)** Main carbonate outcrops along the Mediterranean coasts (orange); location of studied tidal notches (red dots with numbers, Table 2; S1 SM); location of tide gauges (green dots); coastal and submarine springs with outflows higher than 1000 L per second (blue arrows from Civita, 2008). **b)** Tectonic setting of western and central Mediterranean region (modified after Oldow et al., 2002): 1) Water depth >1000, 2) Water depth 0–1000 m, 3) Contractional fault system, 4) Transcurrent fault systems, 5) Extensional fault system. **c)** Holocene and MIS 5.5 vertical tectonic movements along the Mediterranean coasts. Data calculated from: Antonioli et al., 2009; Faivre et al., 2010, 2011; Ferranti et al., 2006, Ferranti et al., 2010, Galili et al., 2011; Pavlopoulos et al., 2012; Radic Rossi and Antonioli 2008, Rodriguez-Vidal et al., 2007; Poulos et al., 2009; Stanley and Toscano 2009; Stewart and Morhange 2009; Tsimplis et al., 2011; Yaltirak et al., 2002; Vött 2007. (For interpretation of the references to colour in this figure legend, the reader is referred to the web version of this article.)



Furlani et al., 2014a). Karst drainage systems can be responsible of high discharges of water, as they represent most often the output point of extensive networks of groundwater conduits. Flows from springs can be perennial, seasonal or intermittent. Most often, in the Mediterranean, their water load follows the seasonal pattern of the rainfall regime. During strong rainfall events, or flash floods due to Cyclonic perturbations, a large number of new springs can be activated (Bonacci et al., 2006). In Fig. 1a we show a map of the coastal and submarine springs with outflow larger than 1000 L per second (Civita, 2008). Although this map is probably biased by a higher concentration of survey in the Italian peninsula, it can give an idea of how widespread are submarine springs along carbonatic coasts. We highlight that the Greek territory is also characterized by a high number of submarine springs (Fleury et al., 2007).

Tides vary from place to place along the coasts of the Mediterranean, depending on many parameters, such as coastal geometry and bathymetry, but in general Mediterranean tides have lower amplitudes with respect to oceanic ones. The average tidal amplitude is about 40 cm, with the exception of exceptional tides observed in the Gulf of Gabes and in parts of the North Adriatic sea, where they may reach amplitudes up to 1.80 m. In other areas, such as in Greece or Sicily, tides are very small, especially near the amphidromic points where the tidal range is almost non-existent. In the vicinity of the Strait of Gibraltar, the Atlantic ocean affects the tides of the Mediterranean, but its influence rapidly declines further east. However, atmospheric conditions may affect the rhythmic tidal rise and fall in sea level, causing larger oscillations or even hide them at all.

### 2.3. Formation of notches

Nearly half of the Mediterranean rock coasts (Fig. 1a) are built of carbonatic rocks (Furlani et al., 2014b) that date back from Mesozoic to Quaternary. Sedimentary carbonate coasts are characterized by a typical set of landforms (Taborosi and Kazmer, 2013), which are related to a combination of physical, chemical, and biological processes. Their relative importance is dependent on the geographical setting and the local conditions. Chemical solution and biological weathering are the driving factors in sedimentary carbonate coasts development in the Mediterranean coasts (De Waele and Furlani, 2013).

In this study we focus on two coastal landforms, typical of carbonate rocks: marine tidal notches and roof notches. We define Marine Tidal Notches (MTNs) the undercuttings found at or near tidal level on carbonatic cliffs with characteristic shaped morphology (Fig. 2a,b,e). MTNs are characterized by both roof and a floor, which is often covered by biological incrustations. In the particular case where the notch lacks a floor, we defined it as Roof Notch (hereafter RN, Fig. 2c). Hereafter we refer in general to 'notches' to indicate both MTNs and RNs. MTNs and RNs are most common on carbonate rocks, although recently Trenhaile (2014) has argued that notches form also as a consequence of wetting and drying cycles in volcanic lahar deposits in Mexico. Focussing on carbonate rocks, four main processes are considered responsible for the formation of notches: biological agents, wetting and drying cycles and salt weathering, hyperkarst processes and mechanical erosion.

#### 2.3.1. Biological agents

Different kinds of organisms live attached to the rock near sea level. In general, bioeroders contribute to the evolution of notches, while encrusting organisms protect it from deepening. The most known bioeroder in the Mediterranean is *Lithophaga lithophaga*, an endolithic bivalve which lives in galleries bored in calcareous rocks by glandular secretions (Morton and Scott, 1980). Another important class of bioeroders are grazers (mainly sea urchins), that play a

major role along coral reef coastlines (Peyrot-Clausade et al., 2000; Spencer and Viles, 2002). In the Mediterranean, Torunski (1979), quantified bioerosion by urchins in  $19 \text{ g CaCO}_3 \text{ m}^{-2}$  for *Paracentrotus lividus*, and in  $295 \text{ g CaCO}_3 \text{ m}^{-2}$  for *Sphaerechinus granularis*. In the Mediterranean, *S. Granularis* erosion rates may vary between 16 and  $210 \text{ g CaCO}_3 \text{ m}^{-2}$  (Sartoretto and Francour, 1997), the higher values corresponding to areas where *S. granularis* is steadily replaced by *Echinus melo*, another large echinoid (Laborel et al., 1961). Lithophaga and echinoids live around mean sea level, therefore they may have a role in shaping the lower part of the notch, which is continuously submerged. Also, when sea level changes, their role remains unchanged. Further bioerosion is caused by endolithic Cyanobacteria (Le Campion-Alsumard, 1979) in the supralittoral zone, together with limpets (*Patella* spp.) and Chitons in the midlittoral zone (Laborel and Laborel-Deguen, 1996).

While bioerosion plays a role in the consummation of rocks in the intertidal zone, some hard bottom communities can protect the bedrock from erosion (Laborel and Laborel-Deguen, 1996; Naylor and Viles, 2002; Spencer and Viles, 2002). In the Mediterranean, constructional (and therefore protective) elements are the rim-building coralline rhodophyte *Lithophyllum lichenoides*, brown algae (*Cystoseira* and *Sargassum*), fixed Vermetid Gastropod Molluscs (*Dendropoma* spp., *Petalocochus* spp.), Cirrhipeds (*Balanus* sp. and *Tetraclita* spp), as well as *Mytilus* sp. and *Ostrea* sp.

#### 2.3.2. Wetting and drying cycles and salt weathering

The importance of these processes in notch formation has been recently highlighted by Trenhaile (2014). In the spray zone, called supralittoral in biological zonation (Laborel and Laborel-Deguen, 1996), haloclastic processes trigger cliff erosion through the penetration of saline water into structural discontinuities of the bedrock and its evaporation, with the subsequent deposition of salt crystals, which can grow from solution, expand due to heating or change their volume due to hydration. These processes lead to modification in the volume of the crystals, which causes an increase of pressure on the walls, triggering the fragmentation of the rock. Another important weathering process along rocky coastlines is associated to wetting and drying cycles (Stephenson and Kirk, 2000; Kanyaya and Trenhaile, 2005; Trenhaile and Porter, 2007). In cold climates, weathering due to frost action plays also a significant role in the upper part of the cliff (Trenhaile and Mercan, 1984).

#### 2.3.3. Hyperkarst

The debate upon the possibility that limestones can be dissolved in seawater lasts since the early 30's (MacFadyen, 1930). Solution of a calcareous rock depends on the saturation of the seawater with respect to calcium carbonate. If the seawater is under saturated in this component with respect to the lithology, then dissolution can occur. This happens in proximity of springs of groundwater (Higgins, 1980) or due to water mixing (Kaye, 1957; Verstappen, 1960) or by surface film effects due to gaseous exchanges with the air (Emery, 1962). Kelletat, 2005, argues that seawater is always oversaturated (in tropical and subtropical latitudes several times supersaturated) by dissolved carbonates and is not able to destroy carbonates by solution. To falsify this hypothesis, Furlani and Cucchi, 2013 collected micro erosion metre data on a vertical limestone slab in the Adriatic Sea and suggested that the shape of the tidal notch is consistent with the distribution of erosion rates along the slab.

#### 2.3.4. Mechanical erosion

While wave abrasion *sensu stricto* (i.e. wave abrasion due to sand or pebbles used as abrasion tools against the rock) plays no part in the development of a tidal notch, mechanical erosion can still



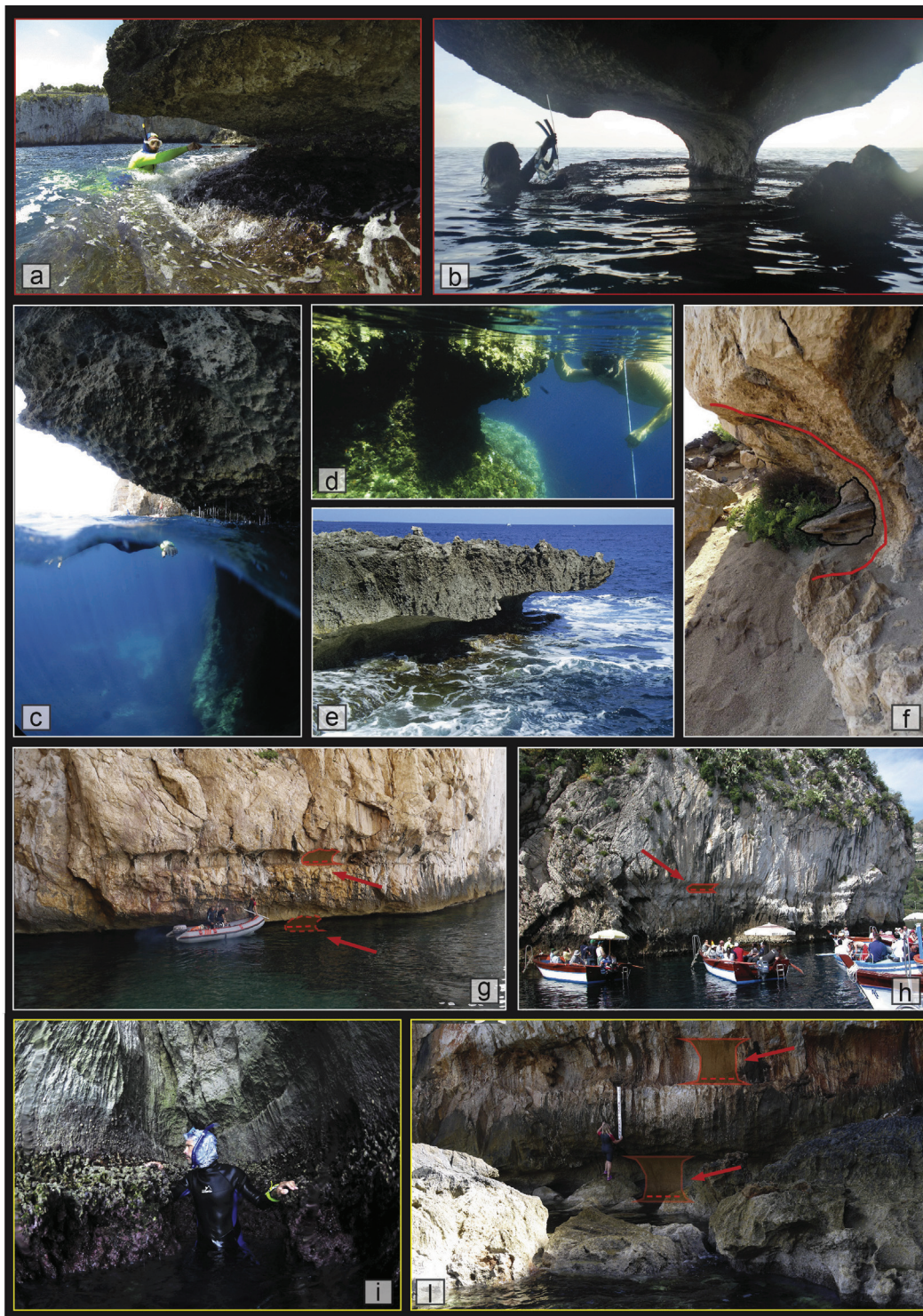


**Fig. 2.** Notches along the central Mediterranean carbonatic coast: **a)** a tidal notch (Zinzulusa, Apulia). **b)** an impressive tidal notch on an isolated limestone rock (Cala Fuili, Sardinia). **c)** a roof notch (Malta) **d)** a submerged notch (Limski canal, Croatia). **e)** a well developed tidal notch carved on the rocky headlands of Favignana. **f)** Eolianite deposit covering the Last Interglacial notch (Biddiriscottai, Sardinia), **g)** Modern and MIS 5.5 tidal notches (Masua, Sardinia), **h)** uplifted tidal notch (Taormina, Sicily), **i)** one metre high corallinae algae in a cul de sac with high pressure splash (Malta) **j)** oversized notch in a cul de sac (Buggerru, Sardinia).

happen in the intertidal to slightly supratidal zone – in function of the deep at the base of the cliff and relatively to the impacting wave features – for two main reasons. First, the resistance of the rock to wave attack is function of its lithology and of the structural discontinuities characterizing it (Kleypas et al., 1999). These can be cracks, cleavages, joints, faults, and bedding planes, some being

inherent in lithology and others being of tectonic origin. Under wave action, the air contained inside the interstices is suddenly compressed, resulting in a pressure increase exerting a stress on the walls of the opening, widening and deepening it until the removal of part of the rock. This process acts in the zone where air and water alternate, i.e. above and below the fluctuating waterline (Trenhaile,



2002). Second, along limestone coastlines, chemical and biochemical dissolution processes happening near tidal level may favour mechanical erosion by influencing the material properties of rock, and weakening or creating joint or boundaries (for details, see Table 4 of [Naylor et al., 2012](#)).

#### 2.4. Rates of erosion in the intertidal zone

What are the rates at which tidal notches are forming? Field measurements of erosion rates in the intertidal zone have been conducted in different areas since the end of the seventies mainly using Micro Erosion Meters (MEM) and Traversing Micro Erosion Meters (TMEM), mostly on shore platforms and sloping limestone surfaces ([Furlani and Cucchi, 2013](#)). [Torunski \(1979\)](#) reported erosion rates in the range of 0.07–1.114 mm/yr from a carbonate intertidal zone of the northeastern Adriatic, which is mainly composed by low-angle plunging cliffs. [Furlani et al. \(2009\)](#) indicated lower values for the supratidal zone (0.09–0.194 mm/yr), and suggested that erosion rates in the supratidal and subtidal zone are one order of magnitude lower than the intertidal zone for the same type of coast. It has been pointed out that seasonal variations are possible in carbonate lowering rates, with higher rates in summer ([Torunski, 1979](#)) and in autumn ([Furlani et al., 2009](#)). A compilation of coastal erosion rates, derived and adapted from [Furlani et al., 2010](#), is presented in the supplementary material (S2 in SM) attached to this publication.

In some cases, such as in the Gulf of Trieste, the lack of the present-day notch and the occurrence of an underwater notch ([Fig. 2d](#)) has been related either to the tectonic subsidence of the area ([Antonioli et al., 2004, 2007](#)) or to temperature variations, such as the Medieval Warm Period where enhanced dissolution was possible. In the Gulf of Trieste, [Furlani et al. \(2010\)](#) estimated erosion rates of limestone surfaces located in the intertidal zone, and on the contribution of seawater and the bioerosion effects to notch development ([Furlani and Cucchi, 2013](#)), using a MEM. [Furlani and Cucchi \(2013\)](#) measured maximum rates up to about 0.3 mm/yr occurring in the mid-intertidal zone. Overall, measurements indicate that lowering rates (that include all the notch formation processes) range from 0.02 to 2.1 mm/yr, a range which contains the rates of bioerosion reported by [Evelpidou et al., 2012](#) of 0.2–1.28 mm/yr.

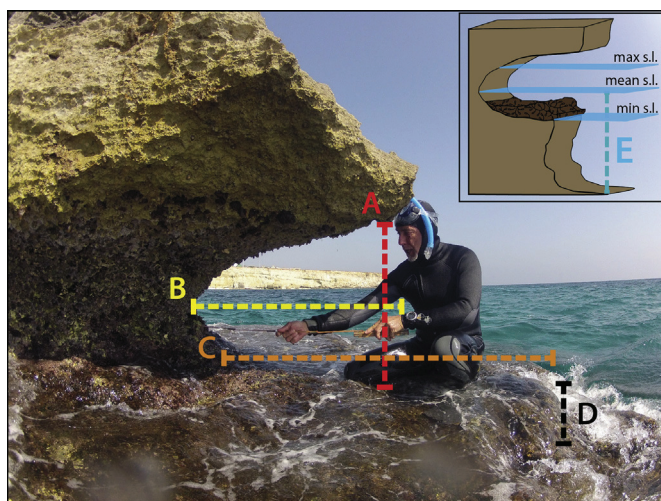


**Fig. 3.** Morphometric measures: A) Average notch width, B) Notch depth, C) Bottom depth (reef when present), D) reef and step (if present) thickness, E) Depth of cliff toe at mean sea level.

### 3. Methods

#### 3.1. Field observations

In this study, we report the results of the survey of the modern notch in 71 out of 73 visited sites along carbonate coastlines in the Mediterranean.

A standardized terminology defining the morphological features of the notches is not available in literature, and often the same measure is reported with different names. To clarify our terminology, we report a graphic view of it in [Fig. 3](#). During our field

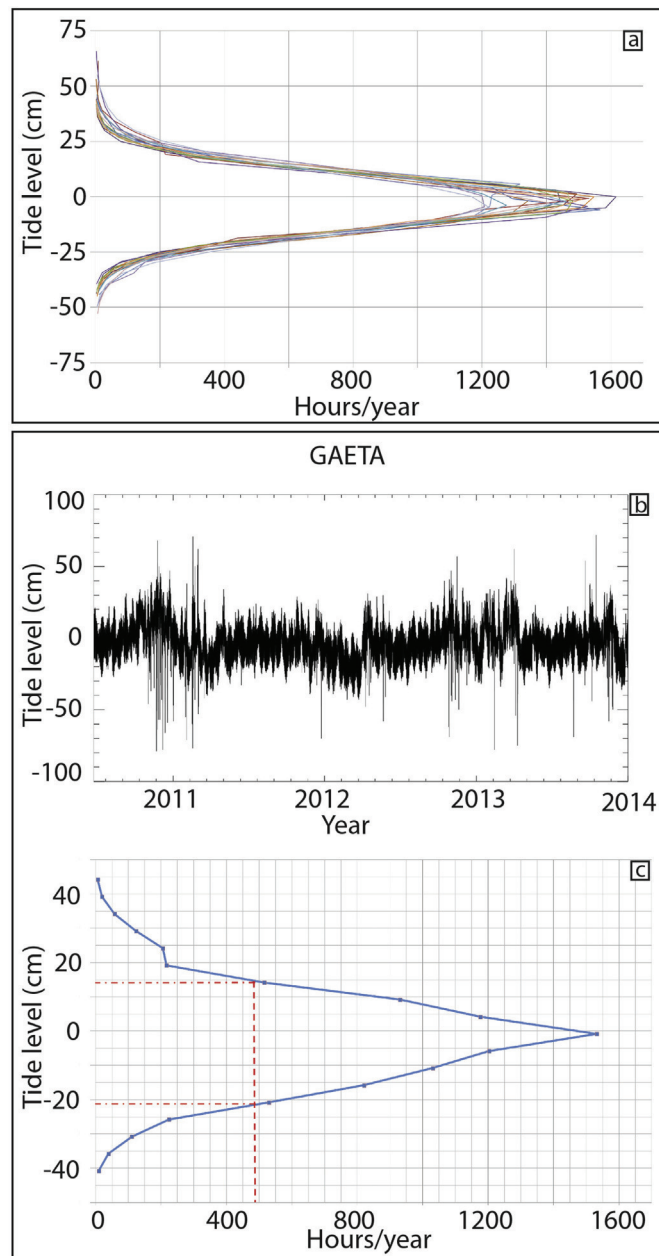


**Fig. 4.** Statistical diagrams of tide gauges data: **a)** height tide trend (hours/year) of the analysed tide gauges: Bari, Naples, Ponza, Catania, Marseille, Elba; Civitavecchia, Gaeta, Carloforte, Cagliari, Imperia, Otranto, Lampedusa, Palermo, Porto Torres, Taranto; **b)** Gaeta tide gauge: tide trend from 2010 to 2014; **c)** Gaeta tide gauge: trend of tide (hours/year, blue line); mean value of significant height tide (vertical axis) and significant hours/year at the same height tide, horizontal axis. (For interpretation of the references to colour in this figure legend, the reader is referred to the web version of this article)

**Table 1**

Data obtained from tide gauges (Fig. 4 for example) and the OSU tidal prediction model, regional solution for the Mediterranean. **1** Station names. **2** lower  $L_{min}$  and upper  $L_{max}$  values of the residual sea level calculated for about 10 h/year. **3** Sum of values on column 2: maximum tide level. **4** Number of hours for year at the histogram maximum (Fig 4), tide level values at half maximum of the histogram (sixth and seventh columns). **5–6** Lower and upper limit at half maximum (cm) of the histogram. **7** Sum of columns 5 and 6. **8** Average notch width cm (see Table 2). We show that overall, the root mean square error between the tidal gauge data and the model data is ~4 cm.

1	2		3	4	5	6		7	8
Tide gauge station <sup>1</sup>	L <sub>min</sub> (cm) <sup>2</sup>	L <sub>max</sub> (cm)	Maximum tidal level	Maximum value of hours/year	Significant hours	Lower and upper value at significant hours (cm)		Mean tide value at half maximum tide level (cm)	Values obtained from OSU tidal model (cm)
Bari	−44.9	55.1	99	1223.38	586.75	−19.9	15.1	35	37.7
Cagliari	−41.2	38.8	80	1510.32	711.05	−16.2	13.8	30	27.9
Palermo	−52.8	42.2	95	1410.15	543.8	−17.8	17.2	35	34.5
Civitavecchia	−41.9	43.1	85	1343.29	549.25	−21.8	13.2	35	—
Carloforte	−38.7	51.3	90	1494.60	588.1	−18.7	11.3	30	28.4
Catania	−40.0	35.0	75	1616.03	617.45	−15.1	14.9	30	23.8
Elba	−40.9	44.1	85	1566.48	647.15	−15.9	14.1	30	32.4
Imperia	−42.1	37.9	80	1481.72	629.8	−17.1	12.9	30	31.2
Lampedusa	−42.2	37.8	80	1442.68	614.15	−17.2	12.8	30	25.6
Marseille	−39.3	55.7	95	1527.65	647.6	−19.3	10.7	30	27.8
Napoli	−43.9	41.1	85	1275.24	563.2	−18.9	16.1	30	38.2
Otranto	−40.0	40.0	80	1547.23	455.6	−20.0	15.0	35	25.8
Ponza	−44.3	35.7	80	1317.40	533.75	−19.2	15.7	35	37.9
Porto Torres	−43.2	36.8	80	1475.44	480.7	−18.2	16.8	35	27.9
Salerno	−49.5	45.5	95	1207.8	439.75	−19.5	20.5	40	38.2
Taranto	−42.2	42.8	85	1461.16	643.35	−17.2	12.8	30	22.1
Gaeta	−40.8	44.2	85	1532.25	485.9	−20.8	14.2	35	37.9
								<b>RMSE</b>	<b>4.08</b>

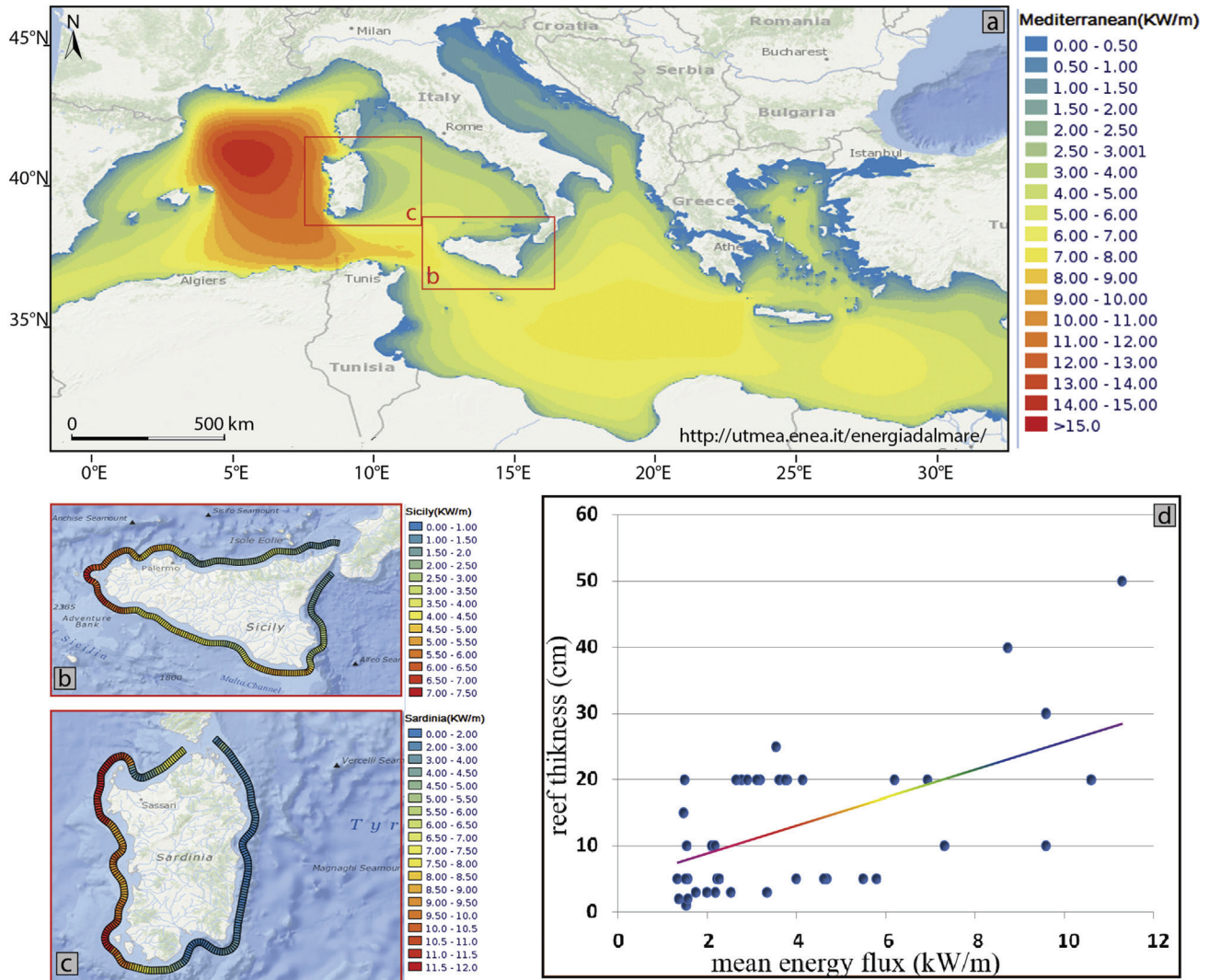


**Fig. 5.** Mediterranean mean waves Energy Flux (kW/m) <http://utmea.enea.it/energiadalmare/> (a). Zoom of mean waves energy flux in Sardinia and Sicily (b and c). Correlation between the rim thickness and mean waves energy flux (d).



**Table 2**

Tidal notches data in Mediterranean Sea **1)** Site number; **2)** Site name; **3)** Type of notch; **4)** Average notch width; **5)** Average notch depth; **6)** Bottom depth of biological rim; **7)** Thickness of biological rim; **8)** Tidal range as predicted by OSU model; **9)** Width of MIS 5.5 notch (if present); **10)** Exposure.

Site N	Site name	Type of notch	Average notch width with uncertainty (cm)	Average notch depth with uncertainty (cm)	Thickness of biological rim with uncertainty (cm)	Tidal range as predicted by OSU model (cm)	MIS 5.5 notch width (cm)	Exposure
1	Colonia de S.Jordie Palma	MTN	55 ± 2.8	90 ± 4.5	2.5 ± 0.1	18.7	—	Exp.
2	Marseille Fausse Monnaie	RN	30 ± 1.5	50 ± 2.5	2.5 ± 0.1	27.8	—	Exp.
3	Balzi Rossi Ventimiglia	MTN	44 ± 2.2	60 ± 10.4	10 ± 0.5	30.5	—	Exp.
4	Noli Malpasso	MTN	100 ± 5	75 ± 25.3	1 ± 0.1	31.2	—	Exp.
5	Capo Caccia	MTN	70 ± 3.5	80 ± 63.1	45 ± 2.3	27.9	0.75	Exp.
6	Porto Conte	MTN	48 ± 2.4	30 ± 1.5	5 ± 0.3	25.8	0.70	Shelt.
7	Porto Conte	MTN	60 ± 3	60 ± 3	10 ± 0.5	23.6	0.70	Shelt.
8	Biddiriscottai	MTN	60 ± 5	70 ± 3.5	10 ± 0.5	34.1	0.80	Shelt.
9	Cala Fuili	MTN	70 ± 4.9	80 ± 160	10 ± 0.5	32.6	0.75	Exp.
10	Sella del Diavolo	MTN	55 ± 2.8	100 ± 5	15 ± 0.8	25.0	—	Exp.
11	Cala Mosca	MTN	50 ± 2.5	190 ± 41.1	15 ± 0.8	27.9	—	Exp.
12	Cala Mosca	MTN	55 ± 2.8	175 ± 26.5	15 ± 0.8	27.3	—	Exp.
13	Masua	MTN	50 ± 2.5	75 ± 6.3	10 ± 0.5	24.5	0.75	Exp.
14	Masua	MTN	60 ± 4.6	140 ± 7	20 ± 1	27.2	—	Exp.
15	Masua	MTN	48 ± 2.4	50 ± 2.5	20 ± 1	28.4	—	Exp.
16	Pan di zucchero	RN	30 ± 1.5	30 ± 1.5	20 ± 1	28.3	—	Exp.
17	Pan di zucchero	MTN	66 ± 3.3	120 ± 20.9	15 ± 0.8	26.7	—	Exp.
18	Pan di zucchero	MTN	50 ± 2.5	60 ± 3	20 ± 1	24.2	—	Exp.
19	Cala Domestica	MTN	48 ± 2.4	50 ± 2.5	5 ± 0.3	28.1	—	Exp.
20	Cala Domestica	MTN	78 ± 3.9	60 ± 3	10 ± 0.5	26.3	—	Exp.
21	Buggerru	MTN	68 ± 3.4	60 ± 3	10 ± 0.5	22.9	—	Exp.
22	Buggerru	MTN	73 ± 3.7	80 ± 4	30 ± 1.5	25.3	0.8	Shelt.
23	Tharros	MTN	72 ± 3.6	60 ± 3	3 ± 0.2	28.9	—	Exp.
24	Talamone	MTN	42 ± 2.1	40 ± 2	2 ± 0.1	32.4	—	Exp.
25	Circeo	No Notch	—	—	15 ± 0.8	36.9	0.26	Exp.
26	Gaeta	MTN	35 ± 1.8	40 ± 2	35 ± 1.8	37.9	0.50	Exp.
27	Capri	No Notch	70 ± 3.5	40 ± 2	15 ± 0.8	38.2	0.70	Exp.
28	Marettimo Harbour	MTN	55 ± 2.8	100 ± 5	5 ± 0.3	26.4	—	Shelt.
29	Marettimo Castello	MTN	60 ± 3	70 ± 3.5	10 ± 0.5	26.8	0.75	Exp.
30	Favignana Cala rossa	MTN	60 ± 3	70 ± 75.1	20 ± 1	27.2	—	Exp.
31	Levanzo	MTN	60 ± 3	40 ± 2	15 ± 0.8	32.0	—	Exp.
32	Levanzo Harbour	MTN	60 ± 3	100 ± 5	15 ± 0.8	29.6	—	Exp.
33	San Vito Castelluzzo	MTN	52 ± 2.6	40 ± 2	5 ± 0.3	35.9	—	Exp.
34	Macari	MTN	55 ± 2.8	45 ± 2.3	5 ± 0.3	35.9	—	Shelt.
35	Zingaro	MTN	50 ± 2.5	200 ± 10	5 ± 0.3	34.7	—	Exp.
36	Scopello	MTN	50 ± 2.5	60 ± 3	5 ± 0.3	32.3	—	Shelt.
37	Palermo Mondello	MTN	60 ± 3	90 ± 4.5	5 ± 0.3	36.4	—	Exp.
38	Palermo harbour	MTN	55 ± 4.5	70 ± 55.1	5 ± 0.3	34.5	—	Exp.
39	Mongerbino	MTN	70 ± 3.5	85 ± 15.6	5 ± 0.3	37.4	0.80	Exp.
40	Cefalù	MTN	70 ± 3.5	125 ± 25.8	5 ± 0.3	37.7	—	Exp.
41	Cefalù	MTN	60 ± 3	80 ± 4	5 ± 0.3	37.7	—	Exp.
42	Siracusa	MTN	60 ± 3	60 ± 3	20 ± 1	23.8	—	Exp.
43	Siracusa	MTN	45 ± 2.3	60 ± 3	20 ± 1	23.8	—	Exp.
44	Siracusa	MTN	60 ± 3	80 ± 4	20 ± 1	23.8	—	Exp.
45	Siracusa	MTN	30 ± 1.5	70 ± 3.5	20 ± 1	23.8	—	Exp.
46	Siracusa	MTN	62 ± 3.1	150 ± 7.5	20 ± 1	23.8	—	Exp.
47	Marzamemi	MTN	55 ± 2.8	80 ± 4	20 ± 1	24.4	—	Exp.
48	Calamosche	MTN	60 ± 3	80 ± 4	20 ± 1	23.9	—	Exp.
49	Gozo	MTN	95 ± 4.8	80 ± 4	5 ± 0.3	21.4	—	Exp.
50	Gozo Eroded mushroom	MTN	70 ± 3.5	90 ± 4.5	5 ± 0.3	21.0	—	Exp.
51	Comino	MTN	60 ± 3	75 ± 3.8	10 ± 0.5	22.4	—	Exp.
52	Malta	MTN	38 ± 1.9	10 ± 0.5	0 ± 0	25.1	—	Exp.
53	Lampedusa Cala Calandra	MTN	35 ± 1.8	50 ± 2.5	0 ± 0	25.6	—	Exp.
54	Lampedusa	MTN	44 ± 2.2	60 ± 3	3 ± 0.2	24.1	—	Exp.
55	Lampedusa	MTN	36 ± 1.8	40 ± 2	3 ± 0.2	25.2	—	Shelt.
56	Marina di Pulsano	MTN	70 ± 3.5	55 ± 2.8	3 ± 0.2	22.1	—	Shelt.
57	Torre Colimena	MTN	60 ± 3	50 ± 2.5	3 ± 0.2	23.2	—	Exp.
58	Serra Cicora	MTN	45 ± 2.3	130 ± 6.5	10 ± 0.5	22.6	—	Exp.
59	Serra Cicora	MTN	45 ± 2.3	174 ± 8.7	10 ± 0.5	23.3	—	Exp.
60	Santa Maria di Leuca	MTN	60 ± 3	150 ± 7.5	20 ± 1	22.4	—	Exp.
61	Santa Maria di Leuca	MTN	80 ± 4	90 ± 4.5	20 ± 1	21.6	—	Exp.
62	Ciolo	MTN	60 ± 3	90 ± 4.5	20 ± 1	24.9	—	Exp.
63	Zinzulusa	MTN	70 ± 3.5	90 ± 4.5	25 ± 1.3	25.0	—	Exp.
64	Badisco	RN	13 ± 0.7	49.5 ± 8.9	0 ± 0	25.8	—	Shelt.
65	Badisco	MTN	50 ± 2.5	30 ± 1.5	5 ± 0.3	25.8	—	Exp.
66	Badisco	MTN	65 ± 3.3	110 ± 5.5	20 ± 1	25.0	—	Exp.
67	Polignano Modugno	MTN	60 ± 3	30 ± 1.5	40 ± 2	33.3	—	Exp.
68	Polignano San Vito	MTN	70 ± 3.5	90 ± 4.5	2 ± 0.1	36.7	—	Shelt.

(continued on next page)

**Table 2** (continued)

Site N	Site name	Type of notch	Average notch width with uncertainty (cm)	Average notch depth with uncertainty (cm)	Thickness of biological rim with uncertainty (cm)	Tidal range as predicted by OSU model (cm)	MIS 5.5 notch width (cm)	Exposure
69	Giovinazzo	MTN	45 ± 2.3	50 ± 2.5	5 ± 0.3	37.7	—	Exp.
70	Tremi	MTN	40 ± 2	40 ± 2	0 ± 0	32.1	—	Exp.
71	Dubrovnik	RN	10 ± 0.5	50 ± 2.5	0 ± 0	39.8	—	Shelt.
72	Montenegro	RN	10 ± 0.5	50 ± 2.5	0 ± 0	35.8	—	Exp.
73	Gavathas	MTN	52 ± 2.6	45 ± 10.3	3 ± 0.2	22.6	—	Shelt.

surveys, we took the following measures: i) the average notch width (A) is the average vertical extent of the notch; ii) inward notch depth (B) is the horizontal extent of the notch; iii) inward bottom depth (C) is the horizontal extent of the notch base (when present, corresponding to the biological rim extent); iv) thickness and main species of the biological rim at the notch base (D, when present); v) Depth of the cliff toe (E).

We measured the dimensions of notches with an invar rod, while the geographic positioning was taken with a GPS Garmin Montana 650T and plotted on Google Earth maps (S1 in SM). All coordinates are expressed as Lat/Long in WGS84 reference system. Accuracy of location is within 10 m. All measurements were taken with calm sea and were referred to mean sea level using the tide gauge data from the nearest tidal stations ([www.idromare.it](http://www.idromare.it); <http://www.ioc-sealevelmonitoring.org/map.php>), including corrections for atmospheric pressure at the time of measurement. Repeating our measures several time at the same site, we estimated an error of 5% (1  $\sigma$ ) in the recorded values. All our field observations are included as supplementary material to this paper.

We documented individual notches with photographs and videos. Part of this documentation is attached as supplementary material to this publication. At each site we also reported bedrock lithology and age from state geological maps. Finally, we reported the elevation above sea level and width of the Last Interglacial notch, when present. These notches have been preserved in most cases thanks to the presence of younger sediments covering them. In addition to tidal notches in the Mediterranean, we also report the measures of 5 notches outside Mediterranean (see Chapter 5.5), done with the same survey techniques described above.

Supplementary video related to this article can be found at <http://dx.doi.org/10.1016/j.quascirev.2015.03.016>.

### 3.2. Tidal ranges

As the availability of tidal records does not cover adequately our measurement sites, we adopted a twofold strategy to include for each observation an estimate of the tidal range. We first analysed the sea level records at 17 stations in the Mediterranean Sea, taken with a sampling rate of one hour. Most data cover about 15 years (Bari, Cagliari, Civitavecchia, Imperia, Marseille, Napoli, Otranto, Palermo, TarantoCarloforte, Catania, Lampedusa, Porto Torres, Salerno). Other tidal datasets span only about 3 years (Gaeta, Ponza and Elba islands). Data from Italian stations have been provided by the Italian tidal network managed by ISPRA ([www.mareografico.it](http://www.mareografico.it)); the Marseille record has been retrieved from the Réseaux de référence des observations marégraphiques (REFMAR, <http://refmar.shom.fr/home>).

To characterize the sea level variability at each station we show the histogram representing the number of hours per year for which a given sea level occurs (Fig. 4). These plots have been built by calculating the residual sea level (LR) obtained by subtracting the temporal mean  $\langle L \rangle$  from the original sea level time series  $L$ :

$$LR = L - \langle L \rangle$$

Then, the interval over which the residual sea level ranges [ $L_{\min}$ ,  $L_{\max}$ ] is divided into  $N$  bins of 5 cm length; the number  $N$  depending on the station.  $N$ ,  $L_{\min}$ ,  $L_{\max}$  values for each station are shown in Table 1. Finally, the number of data points falling into each bin is counted and converted into hours per year.

As the tide gauge stations often were not close to our study sites, we extracted the tidal ranges for all our 73 locations from the Mediterranean regional version of the Tidal Prediction Software developed at the Oregon State University (OTIS, Gary et al., 2002). The model can be considered as a state-of-art tidal model that assimilates most of the available satellite altimetric data (Topex Poseidon, Topex Tandem, ERS) and in situ observations (i.e. tide gauges, ship born ADCP). The Mediterranean model has a resolution of 1/30° (about 3.7 Km) and makes use of the GEBCO 1' database as bathymetry. The model considers the main eight tidal components ( $m_2$ ,  $s_2$ ,  $n_2$ ,  $k_2$ ,  $k_1$ ,  $o_1$ ,  $p_1$ ,  $q_1$ ) that account for more than 99% of the total tidal elevation. In Table 1 we report the values calculated using the model described above at our tide gauges against the values calculated from the tide stations. We obtain differences in the range of ~4 cm (Table 1). We highlight that this number should be taken at face value, as it is possible that some of the data in the tide gauges have been used to develop the tidal model, therefore elements of circularity might be present in our calculations. Nevertheless, we argue that the model produces values of tidal range that are consistent with the tide gauge data available.

### 3.3. Exposure to waves and wave energy

For each site, we used official nautical cartographies and data from oceanographic buoys (<http://utmea.enea.it/energiadalmare/>) to classify the investigated sites in exposed or sheltered. The yearly climatological wave energy flux (in kW/m) associated to our sites (excluding those with roof notches and those repaired in bays or gulfs) has been estimated using the daily data produced by Liberti et al. (2013) for the period 2001–2010. The computed yearly values are shown in Fig. 5a,b,c.

## 4. Results

### 4.1. Notch parameters and bedrock lithology

In this study, we measured the modern notch in 71 out of 73 visited sites along carbonate coastlines in the Mediterranean, as illustrated in Fig. 3 (see also S3). Only at two sites, Circeo and Capri, the notch is absent. The results of our surveys are shown in Table 2, Fig. 6, and contained in full in the supplementary materials (S4). Photographs that illustrate some of the notches are shown in Fig. 2. In average, all the tidal notches we measured are 45–70 cm wide and 40–100 cm deep, although more extreme values are possible.

At all sites, some kind of biological coverage of the notch bottom was found; in this paper we call it 'biological rim', derived from the term 'algal rim' that has been largely used in Mediterranean marine ecology to indicate the rim formed around sea level by coralline algae (Laborel and Laborel-Deguen, 1996). The most

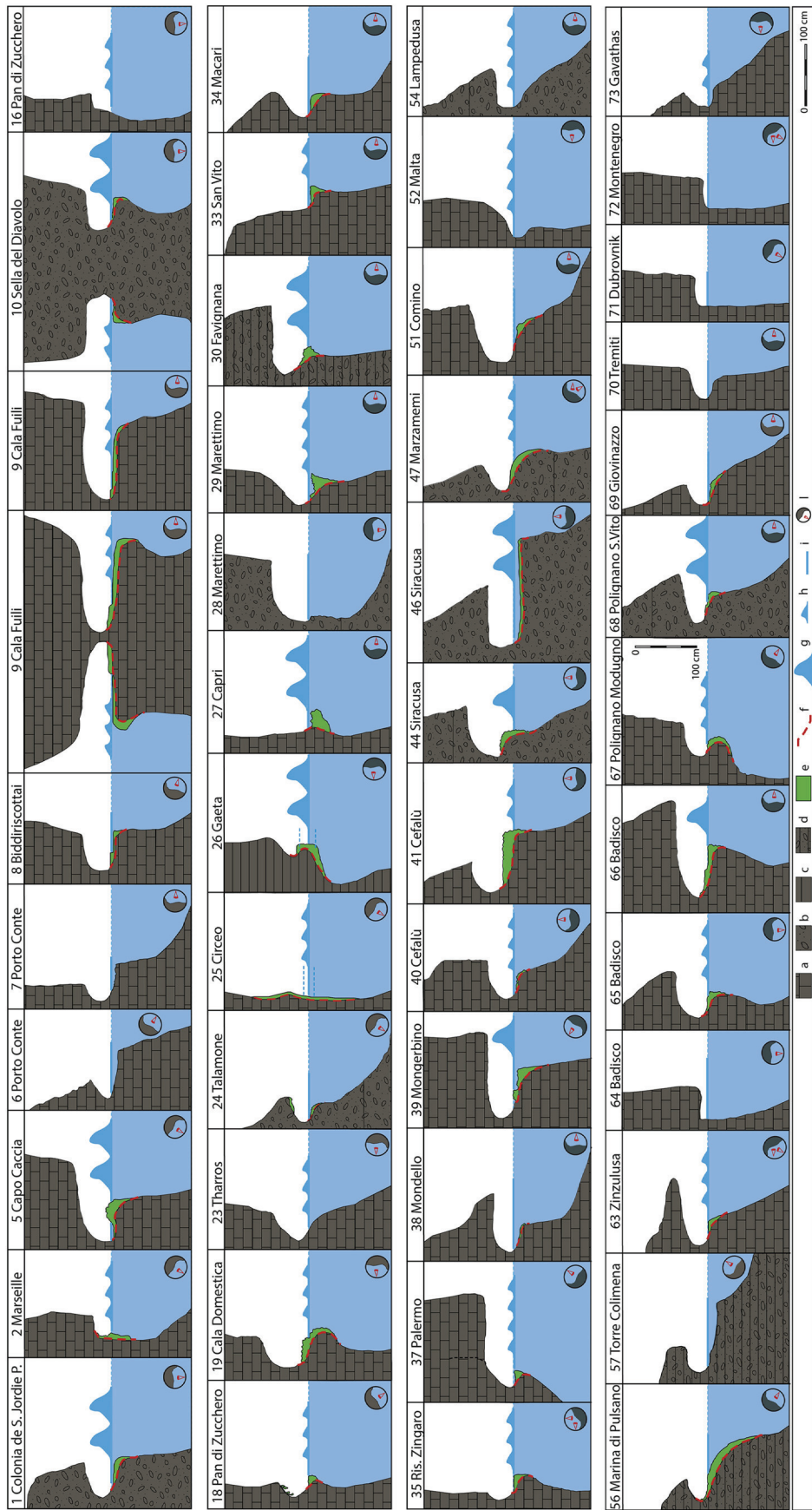


**Fig. 6.** Representative sections of most significant tidal notches studied. a) limestone, b) sandstone and very erosive limestone, c) stratified limestone, d) stratified sandstone and very erosive limestone, e) reef, f) supposed limit between rock and reef. Fetch and kind of sea energy: g) very exposed, h) exposed, i) sheltered. 1) geographical exposure (see Table 2).



**Table 3**  
Geomechanical properties of the rock masses carved by tidal notches.

	Massive limestones	Organogenic limestones	Calclitic dolostones	Dolostones	Calcerenites (sandstones)
Specific Gravity (Gs)	2.65 ÷ 2.73	2.65 ÷ 2.73	2.65 ÷ 2.73	2.65 ÷ 2.73	2.68 ÷ 2.73
Porosity (n%)	4 ÷ 10	10 ÷ 20	10 ÷ 20	4 ÷ 11	44.00 ÷ 50.00
Dry density $\gamma_d$ (KN/m <sup>3</sup> )					12.4 ÷ 15.20
Water absorption (wa %)	2.00	10.00	10.00	4.00	28.40 ÷ 36.20
Uniaxial Compressive Strenght (MPa)	227.51	135.33	131.40	117.67	2.22 ÷ 5.08
Flexural Strengths (MPa)	20.10	16.67	14.51	11.76	1.09 ÷ 8.10

conspicuous coverage is in fact constituted by coralline algae, especially *Lithophyllum* spp., and Vermetids, but in many cases the biological community inhabiting the notch was composed by *Mytilus*, *Patellae*, *Chtamalidae* and *Balanidae*. The biological coverage reaches thicknesses of up to 25 cm.

In general, lithology and relative age of geological units on which notches are carved are different (Fig. 6). As highlighted in Table 3 (see also S5), lithologies in our study area range from Early Cambrian dolomites (Gonnesa Formation) in Sardinia to the Middle Trias (Dolomites of San Pietro dei Monti) in Liguria; from Lower Jurassic – Lias (Inici Formation) at Scopello in Sicily, to Upper Jurassic – Malm (Monte Bardia Formation) at Orosei Gulf and Cefalù Formation in Sicily; from the Cretaceous limestone in Apulia to the Oligocene at Talamone (Brecciole Nummulitiche) and in Apulia (Castro Limestone); from the Miocene (Capraia Formation) at the Tremiti Islands to the Miocene–Pleistocene calcarenites at Favignana island and Jonian Apulia.

As a consequence of the great variability in age, lithology, and development of tectonic, the physic-mechanical characteristics of these rocks are quite different. A broad classification is here done between massive (hard rocks) and calcarenites (that can be defined as “weak rocks”).

4.2. Quantitative relation between notch size, tidal and wave conditions, and bedrock lithology

Comparison of the width of notches located near the tide gauge stations with the tidal data (Fig. 7) highlights that the width of the

notch is always higher than the mean tidal range, but smaller than the maximum and minimum tidal ranges. In order to investigate how width and depth of notches vary between exposed and sheltered sites, we plotted these values against the tidal range calculated using the OSU tidal model described above (Fig. 8a,b,c,d).

In sheltered areas, the notch width is ~0.3–3.2 times the tidal range (Figs. 8c and 7), a ratio that seems maintained in exposed sites (Fig. 8d,e,f), although with larger variability. In exposed sites, the depth of the notch increases with respect to sheltered sites (Fig. 8a,b). This is also evident by comparing notch width and depth. These results highlight that increased wave action results in an increased notch depth rather than an increased notch width, which seems more constant and related, to some extent, to the tidal range and maximum and minimum tidal values (Fig. 7) (Fig. 8c, d, Table 2, S3 SM). We also highlight that the mean tide never exceeds the maximum notch width (Fig. 7). By grouping our data according to lithology, sandstones and stratified limestone have, predictably, a width/depth ratio lower than massive carbonate rocks (Fig. 8g). This relation supports the notion that in weaker lithologies wave action affects notch depth rather than notch width.

Observations of extra-Mediterranean notches seem to fit these quantitative measures. Notches in Barbados, Zanzibar (Tanzania), Bonaire (Netherland Antilles), Phi Phi island (Thailand), Blue Bay and Port Luis (Mauritius) (Fig. 9, Table 4) show that the present notch is always wider than the maximum local tide.

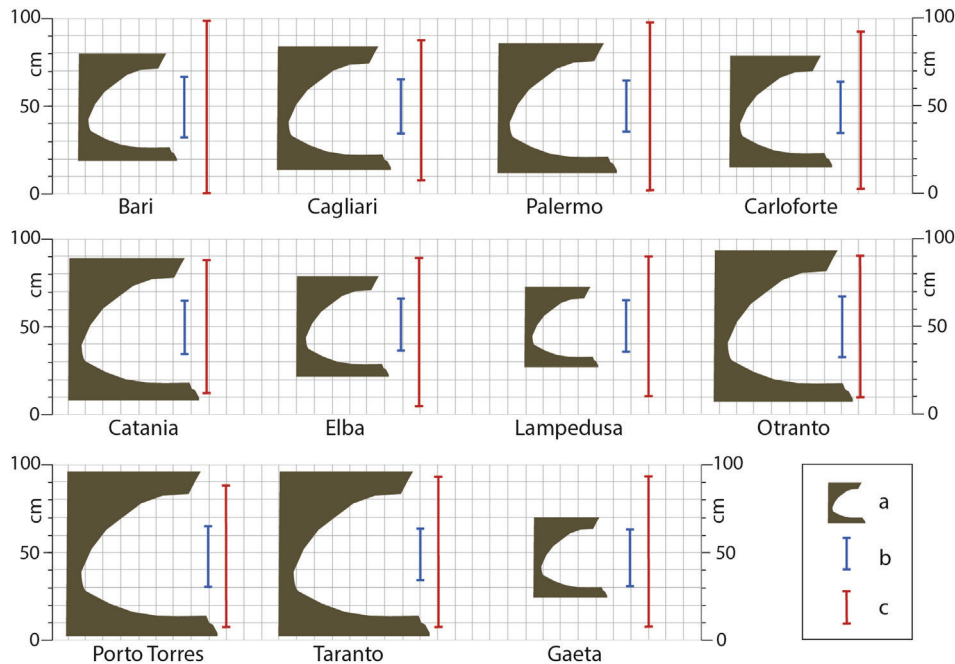


**Fig. 7.** Relationship between notch width (a), mean tide values (b) and extreme (max–min) tide values (c) in locations where notches have been measured near a tide station.